(Received 8 July 2024, Accepted 12 August 2024, Scheduled 25 August 2024)

Compact Dual-Band BPF Based on Loaded SIW with Meandered Slot Line for 5G and Beyond Applications

Hasan AL-Darraji* and Hussam AL-Saedi

Communication Engineering Department, University of Technology, Iraq

ABSTRACT: In this paper, a meandered slot line (MSL) is proposed to miniaturize a substrate-integrated waveguide (SIW) band-pass filter (BPF) and independently realize a dual-band (DB) response. The suggested MSL is symmetrically etched on the upper layer of the SIW resonator; hence, maximum space utilization is realized to increase the miniaturization factor. The TE_{101} and TE_{102} modes were excited and controlled independently through the size and shape of the MLS to highly perturb the electric field distribution inside the SIW cavity. A systematic procedure was employed to design the proposed DB SIW-BPF at the desired specifications. Ansys EDT (2022 R1) full wave simulator was used to analyze and optimize the proposed second-order DB BPF. The suggested filter was fabricated using printed circuit board technology on Rogers RO4003C with a dielectric constant (ε_r) of 3.55. The proposed MSL-SIW structure achieved an overall miniaturization of 68.3% at the lower band compared to the conventional SIW filter, where the resonance frequency of the TE_{101} was shifted from 16.43 GHz to 4.61 GHz. The overall area of the proposed filter is $0.08\lambda_g^2$ at 4.61 GHz with a physical length of 14 mm and width of 7 mm. The operating dual bands are centered at 4.61 GHz for the first band and 6.91 GHz for the second band, with fractional bandwidths of 7.6% and 3.6%, respectively. Measurement results, which highly match the simulation findings, achieved a return loss of 25 dB and 18 dB and an insertion loss (IL) of 0.95 dB and 1.5 dB for the first and second bands, respectively. Accordingly, a simple, low IL, and compact SIW-based BPF was realized, making it an excellent candidate for 5G and beyond applications.

1. INTRODUCTION

Modern wireless communication systems (5G/6G and beyond) support multi-band functionality to provide users with high data rate and low latency services [1–4]. Accordingly, multi-band filter (e.g., dual-band (DB)) is a crucial component in these applications [5, 6]. More specifically, the rapidly increased demand for wireless communication technology leads to the need for high-performance, compact size, and multi-standard band-pass filter (BPF). Planar technology, such as strip and microstrip structures, can be employed, to realize such a filter. Furthermore, substrate-integrated waveguide (SIW), to some extent, may also be incorporated [7–9].

SIW technology employs the advantages of a rectangular waveguide (RWG) in a planar fashion making it suitable for integration within modern systems [10]. As a result, high-performance filters can be created based on SIW technology; nonetheless, SIW structures still suffer from size matter that necessitates additional efforts to overcome such limitations in order to utilize SIW in a wide range of applications. Various methods were employed to miniaturize SIW-based BPFs while at the same time maintaining the advantageous high-performance capabilities of the SIW technology [11].

Modified SIW-based cavity was proposed in various works to realize DB BPFs [12–27]. A study in [12] presented the implementation of a compact DB BPF in an SIW cavity using an embedded co-planar waveguide (ECPW) resonator and a capacitively loaded resonator (CLR), and this filter operated at 8.41 GHz and 14.29 GHz with an area of $0.1\lambda_g^2$. Its insertion loss (IL) was 1.28 dB and 1.91 dB with fractional bandwidths (FBWs) of 21.2% and 7.3%, and return loss (RL) better than 12 dB and 10 dB, respectively. SIW resonator loaded with reduced height vias was proposed in [13] to design a 2nd order compact DB BPF operating at 2.51 GHz and 5.3 GHz. This filter captured an area of $0.35\lambda_g^2$ with three dielectric substrates making it a complex and large size filter. In [14], a transversely electric slot and short-circuited co-planar transmission line were utilized within SIW resonator to realize a DB BPF with FBWs of 2.88% and 4.82% centered at 10.05 GHz and 13.7 GHz, respectively. Furthermore, the presented filter was designed over a large area of $1.1\lambda_g^2$ having ILs of 1.8 dB and 1.4 dB, and $RL > 10$ dB. An E-slot was incorporated with an SIW cavity to achieve a 2nd order DB BPF centered at 3.6 GHz and 6.4 GHz with a filter area of $0.16\lambda_g^2$ [15]. It realized an IL of (1.3 and 1.8) dB, FBW of (3.3% and 2.4%), and RL better than 14 dB. Then, a modified E-shaped slot was used to replace the conventional E-slot where a compact DB BPF with 2nd order was achieved operating at 3.6 GHz and 7.1 GHz with ILs of 1.2 and 1.3 dB, FBWs of 8.2% and 6.7% over an area of $0.084\lambda_g^2$. A complementary split ring resonator (CSRR) loaded on SIW resonator was proposed in [16] to create a 2nd order DB BPF. The TE_{102} and TE_{201} were excited at 7.89 GHz and 8.89 GHz, respectively. The presented filter occupies an area of $0.74\lambda_g^2$ which is a relatively large area; furthermore, the obtained ILs were 1.5 dB and 1.9 dB with the FBWs as 3.42% and 3.93%, respectively.

* Corresponding author: Hasan Al-Darraji (coe.21.21@grad.uotechnology.edu.iq).

A circular SIW resonator loaded with several via posts and slots was presented in [17] to generate a DB BPF centered at 7.71 GHz and 9.64 GHz, but it captured a large area of $1.25\lambda_g^2$. The attained ILs were 1.9 dB and 1.65 dB, and FBWs of 5.45% and 8.1%, respectively; the RL was better than 10 dB. The presented filter was designed with only one resonator. Higher order filter will be a challenge, and the unutilized area in between resonators will be large. A multi-layered SIW was studied in [18] to design a DB BPF. The suggested filter operated at 9.2 GHz and 12.2 GHz over a large filter area of $1.4\lambda_g^2$. Measured ILs were 1 dB and 1.3 dB, FBWs of 12.2% and 9.2%, and RL was better than 17.5 dB, respectively. This type of structure requires a complicated fabrication process that increases the fabrication cost. In [19], a DB BPF operating at 8 GHz and 11.4 GHz was proposed. It utilized different types of resonators, namely dual and single mode SIW resonators to achieve 3rd order DB BPF with wide-stopband rejection. Still, its size is immense where it captures an area of $2.17\lambda_g^2$. The measured filter showed high ILs of 2.26 dB and 3.07 dB, FBWs of 3.01% and 2.46%, and RL better than 15 dB. An SIW DB BPF was proposed in [20] utilizing gap-coupled evanescent-mode. It operated with FBWs of 8.1% and 3.52% centered at 3.7 GHz and 5.96 GHz with filter area of $0.13\lambda_g^2$. Measurement showed ILs of 1 dB and 2.73 dB, and RLs better than 15 dB and 10 dB, respectively. A high selectivity DB BPF was introduced in [21] operating at 9.38 GHz and 13.19 GHz having FBWs, ILs, RL, filter area of 16.53%, 9.94%, 0.57 dB, 1.67 dB, > 14.2 dB, and $0.56\lambda_g^2$, respectively. A DB BPF functioning at the X-band was suggested in [22] by employing dual-modes excited within a half-mode SIW resonator loaded with a T-shaped slot. This filter achieved dual bands centered at 8.67 GHz and 11.52 GHz and FBWs of 3.13% and 1.18%. It was designed over a large filter area of $0.28\lambda_g^2$. The measured ILs were 0.48 dB and 0.31 dB, and RLs were better than 20 dB and 18 dB. Different sizes of metallic vias were utilized in [23] to design a 2nd order DB SIW BPF centered at 17.1 GHz and 19.38 GHz. This filter conquers a large filter area of $2.64\lambda_g^2$. Measurement results revealed that the ILs were 2.1 dB and 1 dB; FBWs were 2.01% and 4.1%; RLs were 21 dB and 17 dB, respectively. In [24], a stacked perturbed circular SIW cavity was presented to realize a DB BPF. A 2nd-order DB BPF operating at 9.89 GHz and 11.98 GHz was proposed by employing two substrates making it a complex structure. It achieved ILs of 1.27 dB and 1.29 dB over a relatively large filter area of $1.144\lambda_g^2$. Furthermore, the filter operates over FBWs of 3.6% and 4.2%, with RL better than 18 dB at both passbands. A multi-mode SIW resonator loaded with centered vias was presented in [25] to realize a DB BPF working at 8.3 GHz and 10.8 GHz over an extremely large filter area of $1.06\lambda_g^2$ attaining ILs of 1.9 dB and 1.7 dB with FBWs of 2.4% and 4.6% and RL better than 19.6 dB. Two substrate layers were utilized to design DB BPFs in [26, 27] realizing 2nd order filter; nonetheless, high IL levels were attained from these filters making them not suitable for low-cost and high-performance applications. Based on the review of state-of-the-art, it is concluded that multi-band BPF based on SIW technology is a promising solution to modern wireless communication systems, but filter size, IL level, bands independency, and complexity are still challenging limitations that require further research and exploration.

In accordance to these necessities, this paper proposes an excellent and affordable solution to bridge the gap between modern technology demands and the SIW-based filters by designing a compact DB BPF to operate at modern wireless communication frequency bands. This filter was constructed by employing SIW resonator loaded with smartly designed modified E-shaped slot as a meandered slot line (MSL) resonator. In this research, a very accurate design method based on insertion loss method, coupling matrix realization, and eigenmode analysis was used to model the proposed filter where the theoretical calculations were validated using full-wave simulator as well as with measured findings. An effective miniaturization level was achieved, and a high degree of independence among operating bands was sustained. Furthermore, the suggested DB BPF was simulated, fabricated, and tested using the Anritsu VNA. Measurement results show that the proposed filter exhibits low IL, compact size, and independent passbands exceeding the reported DB BPF in the literature. In this paper, the utilization of novel MSL structure leads to size miniaturization and bands independency which are the main contribution achieved on the proposed BPF.

2. DB BPF BASED ON LOADED SIW WITH MSL

This section presents the development stages of a 2nd order DB BPF. The proposed filter utilizes an insertion loss design procedure to calculate the theoretical response and essential low-pass parameters of the filter [28]. It is worth mentioning that the design method employed in this paper is typically utilized to design a single band Chebyshev BPF with any order, RL level, FBW, and center frequency (CF); nonetheless, to utilize this method to design a DB BPF, a multi-mode resonator with independent modes control must be used so that superposition theorem can be employed to independently design a compact DB BPF. As a result, the proposed design procedure can be utilized to design a multi-band BPF with any filter order, FBW, and RL level. The specifications of the suggested bands are listed in Table 1. Based on these specifications, the low-pass prototype parameters were determined; moreover, the coupling matrix and group delay (τ) of these bands were also calculated, as shown in Table 2. The calculated low-pass prototype parameters and coupling elements are found to be equal for both bands.

TABLE 1. Specifications of the proposed DB BPF.

Parameter	Value	Parameter	Value
f_{01}	4.6 GHz	RL_1	20 dB
f_{02}	6.9 GHz	RL_2	20 dB
Δ_1	7.6%	N_1	2
Δ_2	3.6%	N_2	2

f_{01} and f_{02} are the center frequencies; Δ_1 and Δ_2 are the FBWs; RL_1 and RL_2 are the return loss levels; and N_1 and N_2 are the orders of the first and second bands, respectively. The coupling matrix [**M**] elements are associated with the FBW.

TABLE 2. Calculated parameters of the proposed DB BPF.

Parameter	Value	Parameter	Value
g_0	1	M_{S1}	1.5
g_1	0.6667	M_{12}	1.6583
g_2	0.5454	M_{21}	1.6583
g_3	1.2222	M_{2L}	1.5
τ_1	1.2126 ns	τ_2	1.6976 ns

Subsequently, M_{ij} is obtained by applying Eq. (1).

$$M_{ij} = \frac{f_0}{BW}\frac{f_m^2 - f_e^2}{f_m^2 + f_e^2} \tag{1}$$

where f_0 is the CF; BW is the operating bandwidth; f_e and f_m are the electrical and magnetic resonance frequencies of the two coupled resonators that can be extracted by eigenmode analysis. Group delay method is a rigorous method, which is usually used in filter design to calculate the required coupling between the input feed line and the first resonator (also, the output feed line and the last resonator) to achieve the required FBW with the best impedance matching as reported in [28]. The value τ is mathematically calculated by the following equation:

$$\tau(\omega_0) = \frac{4}{(\omega_2 - \omega_2)}\frac{1}{R} \tag{2}$$

where R is the normalized input/output impedance, and ω_1 and ω_2 are the limits of the BW.

g_i is the ith low-pass prototype parameter; τ_1 and τ_2 are the group delays of the first and second bands, respectively; M_{ij} is the coupling element between resonators i and j. Moreover, S and L refer to the source and load, respectively. The physical realization of the aforementioned parameters will be introduced in the forthcoming subsections.

2.1. Proposed SIW Resonator

The proposed SIW resonator was built by using a Rogers RO4003C substrate which has a dielectric constant (ε_r) of 3.55, thickness (h) of 0.508 mm and loss tangent ($\tan\delta$) of 0.0027; it has a length (L) and width (W). Furthermore, the diameter of the vias of the SIW cavity is d, and the pitch distance between each two successive vias is p. d was set to be 0.25 mm and by using Eq. (3); p was found to be 0.5 mm; and the effective width (W_{eff}) and length (L_{eff}) can be determined by Eq. (5) and Eq. (6), respectively [29]. The proposed SIW resonator was designed as a square-shaped cavity, as depicted in Fig. 1.

$$p \leq 2d \tag{3}$$

$$f_c = \frac{c}{2W\sqrt{\mu_r\varepsilon_r}} \tag{4}$$

$$W_{eff} = W - \frac{d^2}{0.95 \times p} \tag{5}$$

$$L_{eff} = L - \frac{d^2}{0.95 \times p} \tag{6}$$

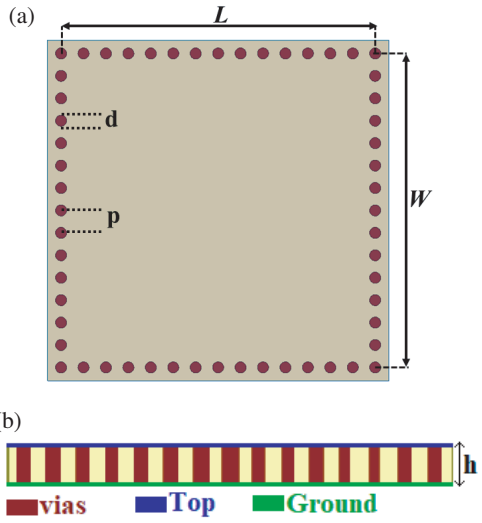

FIGURE 1. Proposed SIW resonator (a) top view and (b) side view.

Eigenmode simulation, a built-in Ansys EDT tool, was used to study the natural first two modes of the SIW cavity, where these modes will be used to design the proposed passbands. It was found that for $L = W = 7$ mm, the SIW resonator supports the TE_{101} and TE_{102} modes at 16.43 GHz and 25.9 GHz, respectively, with an unloaded quality factor (Qu) of 370. The electric field (E-field) distribution of these modes is shown in Figs. 2(a) and 2(b), respectively. These modes can be excited from the same side, and yet different perturbation mechanisms can be employed to independently adjust their frequencies where TE_{101} can be highly perturbed if the SIW resonator is loaded at the middle, whereas the TE_{102} mode can be adjusted if the perturber structure is located closer to the corners of the SIW cavity. This resonator will be used in the next subsections to develop the final resonator. Slot resonator can be used as a simplified technique to load the SIW cavity in order to perturb its modes; hence, decrease of the resonance frequencies can be achieved that yields a miniaturization effect.

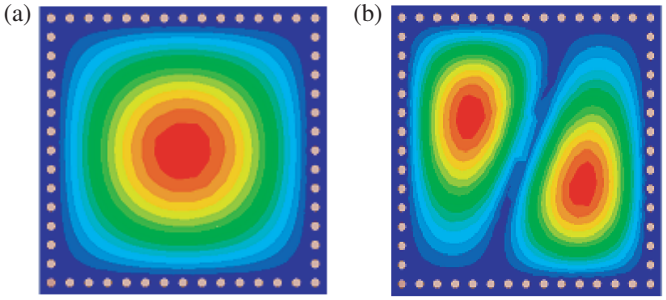

FIGURE 2. E-field distribution of (a) TE_{101} mode and (b) TE_{102} mode.

Proper choice of the shape and dimensions of such a slot can significantly reduce the resonance frequency, and it can afford independent control of these modes.

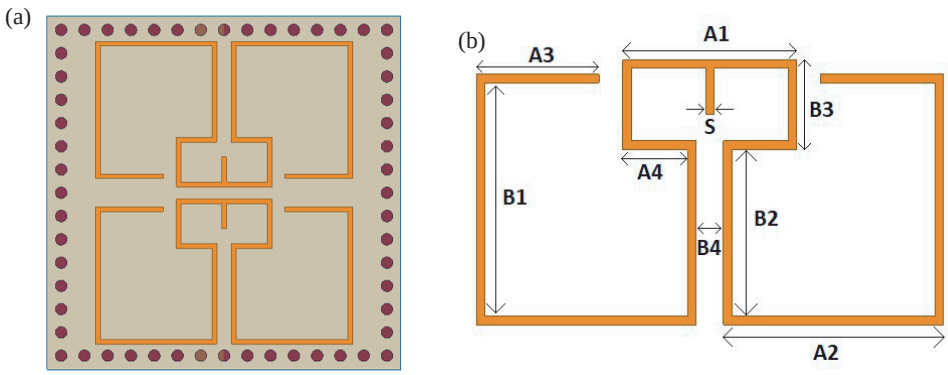

FIGURE 3. The Proposed SIW loaded with MSL (a) top view of the proposed resonator and (b) MSL parameters.

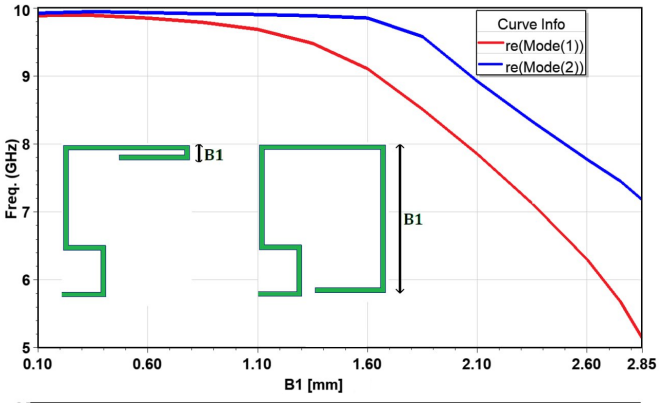

FIGURE 4. Resonance frequencies variation vs. $B1$.

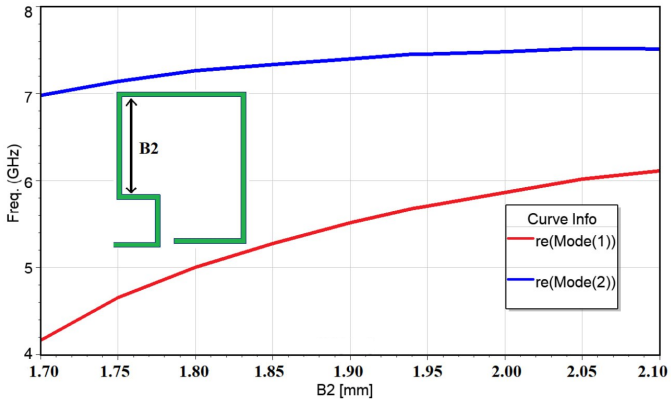

FIGURE 5. Resonance frequencies variation vs. $B2$.

2.2. Proposed SIW Resonator Loaded with MSL

The top layer of the SIW can be used efficiently to be loaded by a slot-like resonator to miniaturize the overall size. This slot functions as a control mean and a miniaturization structure whereby such effects can be utilized in specific shapes and locations. One of the most suitable choices is to use an MSL. In this paper, a modified E-shaped MSL is incorporated to reduce the overall filter size and to drastically shift down the resonance frequencies of the TE_{101} and TE_{102} modes. The modified E-shaped MSLs act as two $\lambda_g/2$ resonators, which load the SIW cavity, with electrically large size due to the meandering effect; hence, a significant miniaturization was achieved within the proposed structure. The SIW cavity was loaded with two symmetrical MSLs. Two identical MSLs were used for two main reasons: firstly, since an SIW cavity has multi-modes where each mode has a different field distribution, the usage of two different meander slots allows more degree of freedom to strongly perturb the largest number of these modes independently. Secondly, it helps to further miniaturize the cavity resonator by cutting the original one into two halves, thus, creating a half-mode resonator with minimum modifications of the original resonator. Fig. 3(a) demonstrates the incorporation of the MSL within the SIW resonator, and Fig. 3(b) displays the design parameters of the proposed MSL. To understand the impact of the MSL, a number of eigenmode analyses were performed by varying the geometric parameters of the proposed MSL.

The impact of parameter $B1$ on the first two-resonance modes (f_{r1} and f_{r2}) is illustrated in Fig. 4. The variation of B1 from 0.1 mm to 2.85 mm decreased f_{r1} and f_{r2} from 9.88 GHz and 9.92 GHz to 5.13 GHz and 7.17 GHz, respectively.

This interval can be divided into two ranges. The first range of $B1$ was between 0.1 mm and 1.6 mm; in this interval, as $B1$ increased, f_{r1} decreased to 9.1 GHz while f_{r2} was slightly reduced to 9.85 GHz. Additionally, as $B1$ rose from 1.6 mm to 2.85 mm, both f_{r1} and f_{r2} were reduced sharply. It can be understood from this behavior that parameter $B1$ can substantially miniaturize the proposed SIW-MSL resonator, and in some regions, it can be used to tune the first mode while the second mode stays unchanged. However, $B2$ showed an opposite performance as that shown in $B1$, where increasing $B2$ resulted in a significant increase in f_{r1}, while f_{r2} was marginally escalated. $B2$ was varied from 1.7 mm to 2.1 mm, causing f_{r1} to increase from 4 to 6 GHz, and f_{r2} to go up from 7 GHz to 7.5 GHz as depicted in Fig. 5.

On the contrary, $B3$ influenced f_{r2} while f_{r1} stayed in a plateau state, as demonstrated in Fig. 6. $B3$ changed from 0.5 mm to 1.1 mm, resulting in shifting down f_{r2} from 9.5 GHz to 7 GHz, while over the same interval of $B3$, f_{r1} stayed at 5.5 GHz.

The optimal dimensions of the proposed MSL were $A1 = 2.06$ mm, $A2 = 2.6$ mm, $A3 = 1.45$ mm, $A4 = 0.77$ mm, $B1 = 2.75$ mm, $B2 = 1.96$ mm, $B3 = 1.06$ mm, and $B4 =$

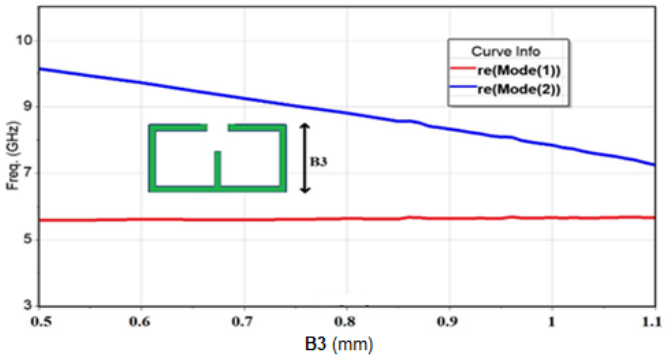

FIGURE 6. Resonance frequencies variation vs. $B3$.

0.32 mm. The MLS was positioned away from the symmetry line on the SIW with a distance of 0.13 mm, and its width (S) was 0.26 mm. Eigenmode simulation was performed on the finalized SIW-MSL resonator to evaluate the resonance frequencies and quality factors. The 1st mode resonates at 5.67 GHz with $Qu = 742$, and the 2nd mode resonates at 7.45 GHz with $Qu = 767$, respectively, as depicted in Fig. 7. Consequently, significant miniaturization was attained for both modes with an enhanced quality factor that impacts the loss level of the suggested SIW-MSL resonator.

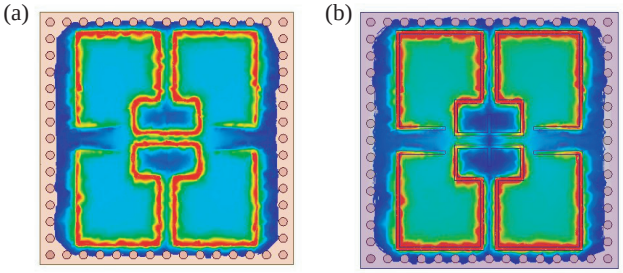

FIGURE 7. E-field distribution (a) 1st resonance mode and (b) 2nd resonance mode.

2.3. Inter-Resonator Coupling

A band-pass filter usually comprises multiple adjacent resonators, and the coupling between them affects its BW and other design characteristics. This coupling can be in the form of an iris or post located between the interconnecting resonators. The iris (or the post) influence is achieved by controlling the power transferred between the coupled resonators. The calculation of the physical dimensions of the gap (g) may be done based on the magnitude of the coupling, as shown in Fig. 8, where g was varied, and M was calculated. It is necessary to use this value in the experimental implementation. With the help of the Ansys EDT simulator, eigenvalues of the coupled resonators can be computed. In the design of SIW filters, the inter-resonator coupling can be determined by directly analyzing the M-parameter since the inter-resonator coupling is achieved by implementing the opening gap in the via walls located in between the two adjacent resonators. The coupling matrix M of two SIW-MSL resonant cavities has been analyzed to achieve optimal g opening that matches the calculated M. The

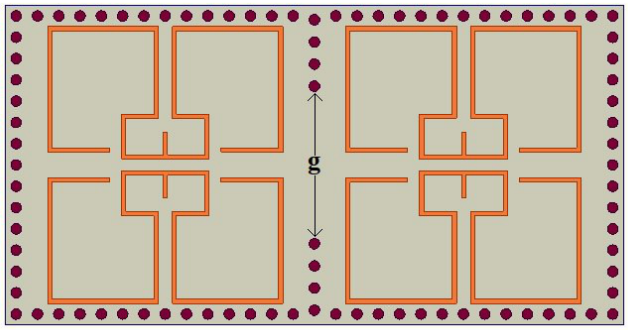

FIGURE 8. Two adjacent resonators separated by vias wall with opening window (g).

coupling strength between SIW-MSL walls may be adjusted by modifying the g to alter the coupling matrix of the cavities.

In Fig. 9, a plot shows the relationship between the g size and coupling value. The coupling matrix for the 1st band is denoted as M_1, and the coupling matrix for 2nd band is denoted as M_2. Both are the passband coupling matrix elements of the filter. As g increases, M_1 and M_2 increase as well, but a small difference between these factors will result in a slight variation in the performance of the proposed BPF at both bands. The parametric study was continued until g reaches a value of 3.2 mm, which is a compromise between the two bands to achieve the best acceptable M_{12} as listed in Table 2.

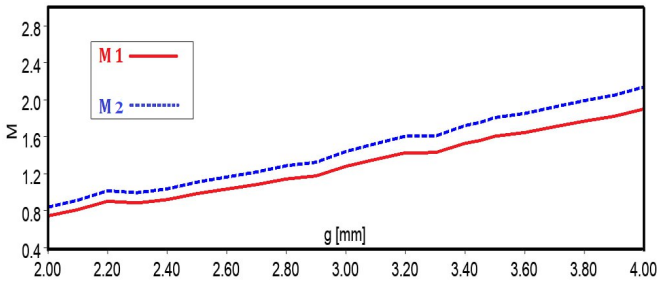

FIGURE 9. Simulated M vs. different g values.

2.4. Input/Output Coupling

The first two resonance modes of the SIW-MSL cavity were located at 5.67 GHz and 7.45 GHz, respectively. The filter's input and output 50-ohm microstrip lines have W_f of 1.136 mm. It is essential to accurately establish the microstrip feed line's size to achieve optimal coupling with the SIW resonator. This feed line serves as a transitional structure between the source and resonator. The group delay method is an excellent technique to assert the input coupling to the resonator. The inset feed structure shown in Fig. 10 is a suitable structure to match the microstrip feed line to the SIW resonator and to adjust the power flow from the source to BPF or from the filter to the load. Fig. 11 shows the variation of the inset width to realize the best-compromised τ for both operating bands. It is found that $\tau_1 = 1.21$ ns, and $\tau_2 = 1.69$ ns. The optimal dimensions of the inset-fed structure were $L_s = 2$ mm, $W_s = 1.1$ mm, $W_f = 1.136$ mm, $v = 0.23$ mm, $u = 0.4$ and $d_v = 0.33$ mm.

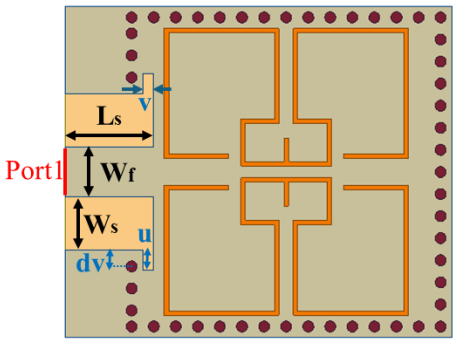

FIGURE 10. Input and output feeding mechanism of top view of the structure.

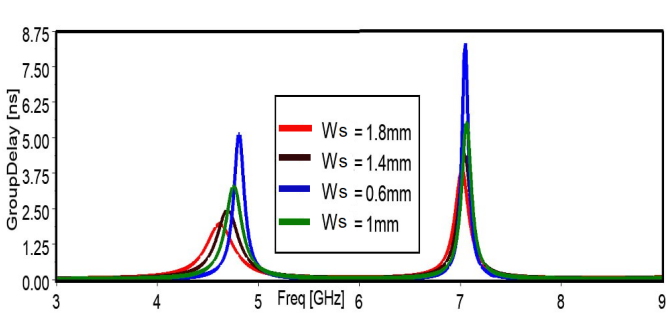

FIGURE 11. Group delay variation of the first and second modes.

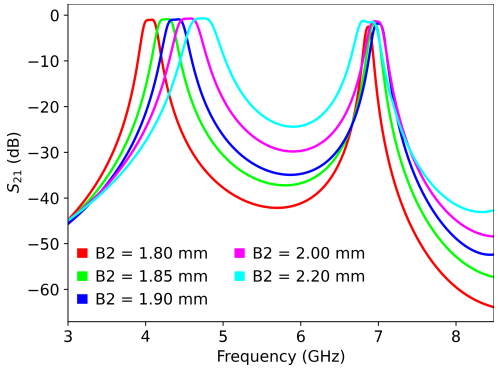

FIGURE 12. Independency analysis of the proposed SIW-MSL BPF (a) first band variation due to $B2$.

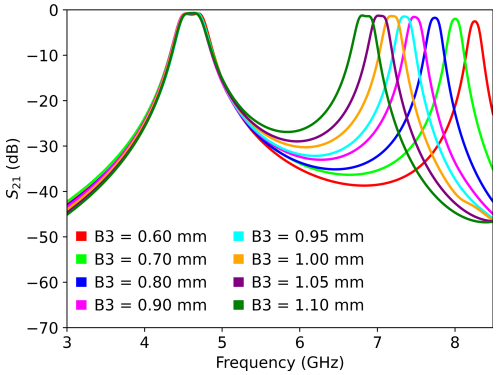

FIGURE 13. Independency analysis of the proposed SIW-MSL BPF second band variation due to $B3$.

3. PROPOSED FILTER ANALYSIS

The optimized components of the proposed filter were connected together to build the final filter. To investigate the independence of each passband, two parametric studies were done separately, and the findings are illustrated in Figs. 12 and 13. The first analysis, as shown in Fig. 12, was executed by varying $B2$. It can be noticed that f_{r1} changes accordingly and independently, while f_{r2} stays the same. On the other hand, the second analysis was done by varying $B3$, meanwhile f_{r1} stayed at the same value, and f_{r2} altered subsequently and independently as illustrated in Fig. 13.

To ensure a reflection-free flow of electromagnetic waves at both terminals of the filter, a necessary step was taken to modify the width and length of the inset feed. In addition to that, to achieve optimal coupling between the resonators of the filter that fits within the specifications of the filter BW, the gap between the coupled resonators was adjusted to take into consideration the impact of connecting the filter's components together. Fig. 14 shows the proposed SIW-MSL BPF structure with parameters under study noted as v, u, L_s, W_s, and g.

The optimized parameters of the proposed filter are demonstrated in Table 3. The optimized value of g was set to be precisely at 3.2 mm. The overall size of the 2nd order DB SIW-MSL BPFs was 7 mm $\times$ 14 mm.

The realized bands were centered at 4.61 GHz and 6.91 GHz, and the RL was determined to be better than 20 dB. The IL at

TABLE 3. Optimal dimensions of proposed DB BPF in (mm).

Para.	Value	Para.	Value	Para.	Value	Para.	Value
L	14	W	7	d	0.25	P	0.5
$A1$	2.06	$A2$	2.6	$A3$	1.45	$A4$	0.77
$B1$	2.75	$B2$	1.96	$B3$	1.06	$B4$	0.32
L_s	2	W_s	1.1	W_f	1.136	g	3.2
v	0.23	u	0.4	dv	0.33	h	0.508

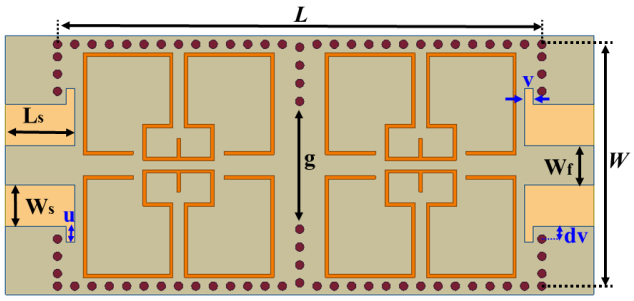

FIGURE 14. Proposed SIW-MSL BPF.

the first passband was found to be 0.68 dB, while it was 1.17 dB at the second passband, as shown in Fig. 15.

The 3-dB BW was about 0.35 GHz equivalent to a FBW of 7.6% at the lower passbands, while it was about 0.25 GHz

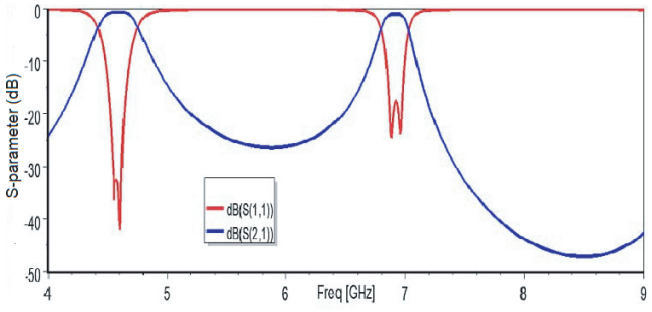

FIGURE 15. Proposed SIW-MSL BPF Simulated S-parameters.

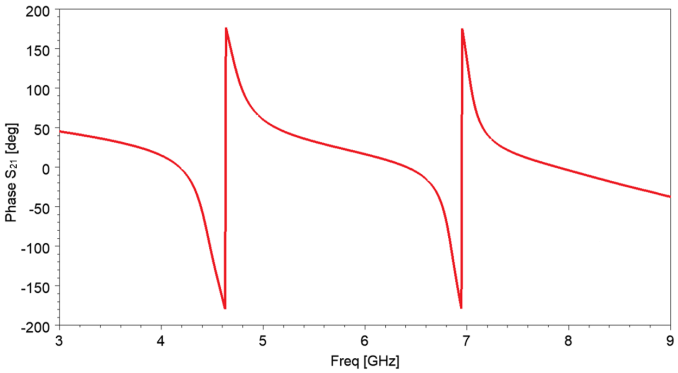

FIGURE 16. Proposed SIW-MSL BPF simulated phase.

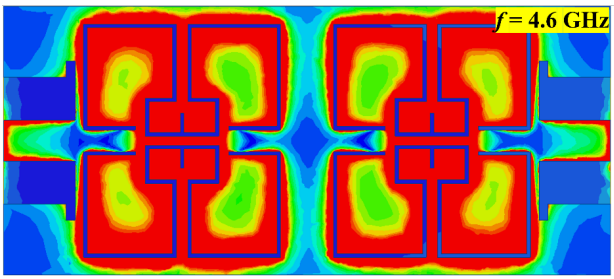

FIGURE 17. Simulated E-field distribution at 4.6 GHz.

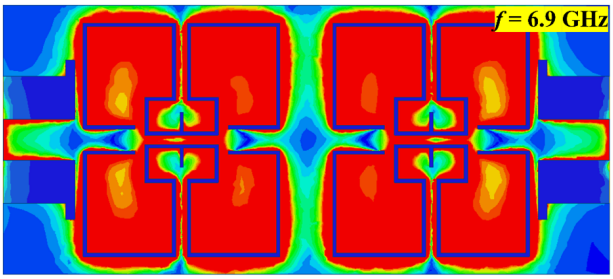

FIGURE 18. Simulated E-field distribution at 6.9 GHz.

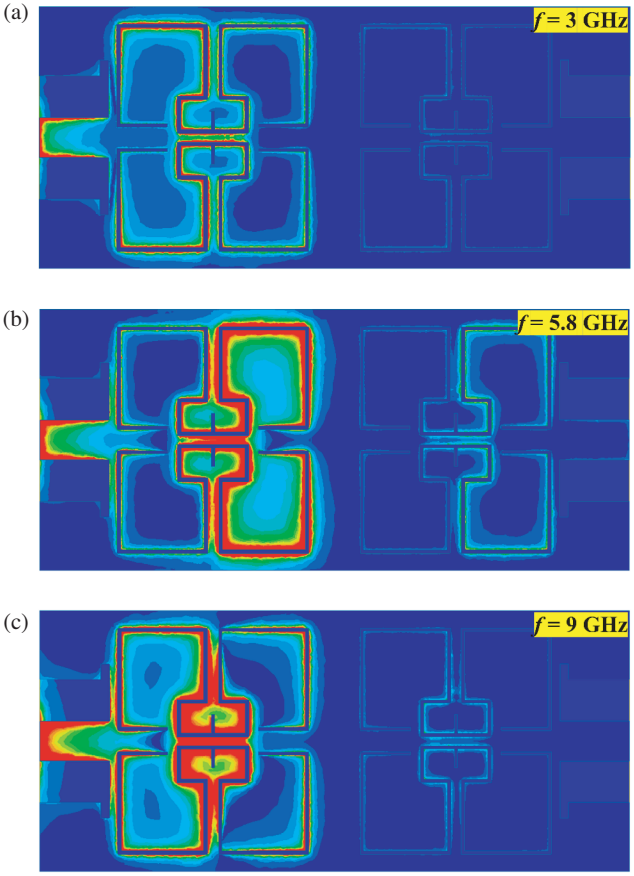

FIGURE 19. Simulated E-field distribution at various frequencies (a) 3 GHz, (b) 5.8 GHz, and (c) 9 GHz.

equivalent to an FBW of 3.6% at the upper passband. Moreover, Fig. 16 displays the phase response of the proposed filter.

The E-field distribution throughout the proposed filter was plotted at different frequencies to further validate the operation principle. Figs. 17 and 18 illustrate the E-field at 4.6 GHz and 6.9 GHz, respectively. It can be seen from these figures that the E-filed passes through the filter from input to output with minimal reflection at the frequencies of 4.6 GHz and 6.9 GHz which are the CFs of the passbands. On the contrary, most of the E-filed was reflected at frequencies equal to 3 GHz, 5.8 GHz, and 9 GHz as demonstrated in Figs. 19(a), (b), and (c).

4. SIMULATION AND MEASUREMENT OF THE PROPOSED SIW-MSL BPF

The fabricated circuit of the proposed 2nd order SIW-MSL BPF is shown in Fig. 20, where a 1-Yuan Chinese coin with a diam-

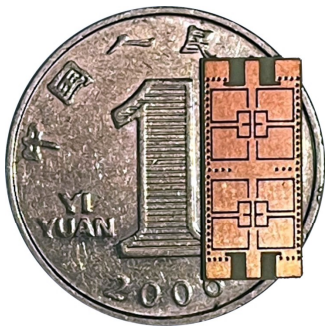

FIGURE 20. Fabricated circuit of the proposed SIW-MSL BPF.

TABLE 4. Comparison of the proposed DB BPF with state-of-the-art.

Ref.	Technology	f_0 (dB)	FBW (%)	IL (dB)	RL (dB)	Size (λ_g^2)	Independency	No. of Layers
[12]	CLR SIW	8.41/14.29	21.2/7.3	1.28/1.91	> 12	0.1	No	1
[13]	Capacitively loaded SIW	2.51/5.3	6.8/5.8	1.41/1.88	> 17	0.35	Yes	3
[14]	Via-post SIW	10.05/13.7	2.88/4.82	1.8/1.4	> 10	1.11	Yes	1
[15]	E-slot SIW	3.6/7.1	8.2/6.7	1.2/1.3	>14	0.084	Yes	1
[16]	CSRR SIW	7.89/8.89	3.42/3.93	1.5/1.9	> 12	0.74	No	1
[17]	Via-post SIW	7.71/9.64	5.45/8.1	1.9/1.65	> 10	1.25	Yes	1
[18]	Multi-layer SIW	9.2/12.2	12.2/9.2	1/1.3	> 17.5	1.4	Yes	2
[19]	Modes suppression-SIW	8/11.4	3.01/2.46	2.26/3.07	>15	2.17	No	1
[20]	Gap-coupled SIW	3.7/5.96	8.1/3.52	1/2.73	> 15	0.13	Yes	1
[21]	Combline resonator-SIW	9.38/13.19	16.53/9.94	0.57/1.67	> 14.2	0.56	Yes	1
[22]	T-Slot SIW	8.67/11.52	3.13/1.18	0.48/0.31	> 20	0.28	No	1
[23]	Via-post SIW	17.1/19.38	2.01/4.1	2.1/1	> 17	2.64	Yes	1
[24]	Circular SIW	9.89/11.98	3.6/4.2	1.27/1.29	> 18	1.14	No	2
[25]	Via-post multi-mode SIW	8.3/10.87	2.4/4.6	1.9/1.71	> 19.6	1.06	No	1
[26]	Folded QMSIW	3.6/5.8	6.4/5.3	2.37/3.74	> 10	0.71	Yes	2
[27]	SIW+Patch	6.97/7.46	2.04/3.26	2.82/2.23	> 15.41	0.69	Yes	2
This work	MSL-SIW	4.61/6.91	7.6/3.6	0.96/1.5	> 18	0.08	Yes	1

eter of 25 mm has been used to reference the size of the proposed BPF. It can be clearly noticed that the proposed BPF has a smaller size than the coin. In reference to λ_g of f_{r1}, the filter has an area of $0.08\lambda_g^2$. The fabricated prototype was analyzed using Anritsu MS4642A vector network analyzer (VNA), as shown in Fig. 21.

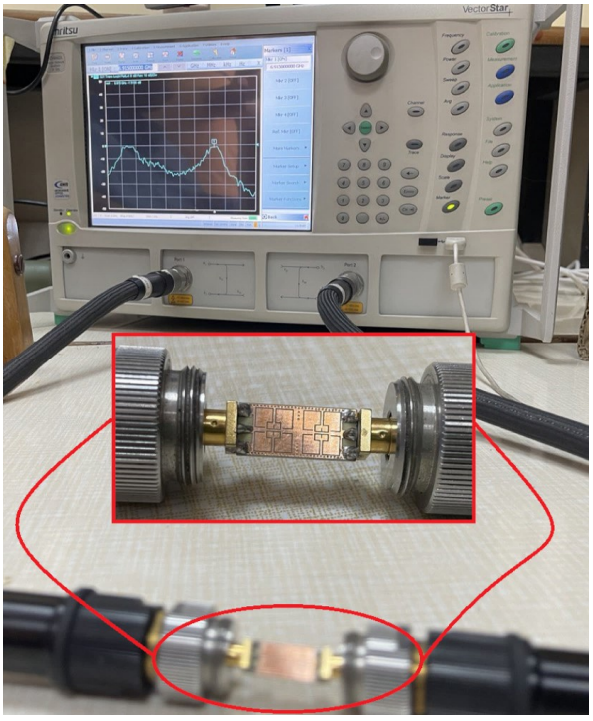

FIGURE 21. Measurements setup.

The validation of the design can be shown through the measurement results in Fig. 22. The results exhibit that the filter's response has two passbands. The first band has a CF of 4.61 GHz and 350 MHz as 3-dB BW (FBW of 7.6%). The RL is better than 23 dB with an IL about 0.96 dB. Additionally, the second band operates at a CF of 6.91 GHz with 250 MHz as 3-dB BW (FBW of 3.62%). The $RL > 18$ dB with an IL about 1.51 dB. The difference in IL level at the two bands is attributed to the impedance matching level at these bands where the first band shows an S_{11} level around 23 dB while the second band shows a lower impedance matching level of $S_{11} = 18$ dB. Furthermore, as the second band operates at higher frequency band centered at 6.91 GHz, the electrical length of the filter is larger than its electrical length at the first band which is centered at 4.61 GHz, so it is natural to experience higher IL level at the higher operating band. Accordingly, the two factors contribute to the increase of the IL in the second band. However, a better matching may enhance the IL. It is worth mentioning that the slight deviation between the simulated and measured outcomes resulted from the effect of the fabrication tolerances, material uncertainty, and assembly misalignment.

Table 4 compares the proposed DB BPF and state-of-the-art DB SIW filters. To ensure fair comparison, only second order filters are listed in the table, where all the listed filters have the same order number of 2. By inspecting this table, it can be easily concluded that the proposed filter captures a smaller area than state-of-the-art besides its good IL level. Accordingly, this research proposes a novel MSL approach to reduce the filter size as well as attain bands tuning separately making it a very competitive structure surpassing available solutions.

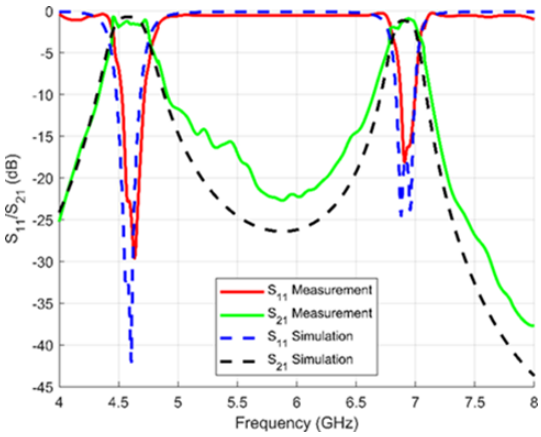

FIGURE 22. Measured and simulated S-parameters of the proposed SIW-MSL BPF.

5. CONCLUSION

This paper has introduced a new design for a compact SIW-based filter. The fundamental idea was to generate two operational passbands that were significantly lower than the waveguide's cutoff frequency. The work was accomplished by meticulously configuring the MSL resonator utilized as the fundamental component of the circuit. The proposed circuits demonstrated desirable characteristics, including cost-effectiveness, easy integration capabilities, and minimal IL, all confirmed through experimental validation. The filter operates at frequencies of 4.61 GHz and 6.91 GHz with FBWs of 7.6% and 3.6% for the first and second passbands, respectively. The measured ILs at these frequencies were 0.96 dB and 1.51 dB, respectively. The filter was manufactured in a compact size of 7 mm $\times$ 14 mm equivalent to $0.08\lambda_g^2$. Due to its properties of a small-sized footprint and high-performance capability, the proposed filter is well suited for DB applications in advanced communication systems.

REFERENCES

[1] Alkhafaji, A. N., A. J. Salim, and J. K. Ali, "Compact substrate integrated waveguide bpf for wideband communication applications," in *Progress In Electromagnetics Research Symposium Proceedings*, 135–139, Prague, Czech Republic, 2015.

[2] Al-Saedi, H., J. A. Attari, W. M. A. Wahab, R. Mittra, and S. Safavi-Naeini, "Single-feed dual-band aperture-coupled antenna for 5G applications," in *2018 18th International Symposium on Antenna Technology and Applied Electromagnetics (ANTEM)*, 1–2, Waterloo, ON, Canada, 2018.

[3] Hong, W., Z. H. Jiang, C. Yu, D. Hou, H. Wang, C. Guo, Y. Hu, L. Kuai, Y. Yu, Z. Jiang, Z. Chen, J. Chen, Z. Yu, J. Zhai, N. Zhang, L. Tian, F. Wu, G. Yang, Z.-C. Hao, and J. Y. Zhou, "The role of millimeter-wave technologies in 5G/6G wireless communications," *IEEE Journal of Microwaves*, Vol. 1, No. 1, 101–122, 2021.

[4] Jiang, W., B. Han, M. A. Habibi, and H. D. Schotten, "The road towards 6G: A comprehensive survey," *IEEE Open Journal of the Communications Society*, Vol. 2, 334–366, 2021.

[5] Zhao, K. and D. Psychogiou, "Three dimensional printed vertically-stacked single-/multi-band coaxial filters and RF diplexers," *IEEE Transactions on Microwave Theory and Techniques*, Vol. 71, No. 11, 4957–4968, 2023.

[6] Li, D., W. Luo, X. Chen, Y. Liu, K.-D. Xu, and Q. Chen, "Miniaturized dual-/tri-/quad-band bandpass filters using perturbed multi-mode SIW cavity," *IEEE Transactions on Components, Packaging and Manufacturing Technology*, Vol. 13, No. 10, 1685–1693, 2023.

[7] Liu, Q., D. Zhou, X. Wang, M. Tang, D. Zhang, and Y. Zhang, "High-selective bandpass filters based on new dual-mode rectangular strip patch resonators," *IEEE Microwave and Wireless Components Letters*, Vol. 31, No. 10, 1123–1126, 2021.

[8] Khani, H. I., A. S. Ezzulddin, and H. Al-Saedi, "Design of a compact and highly independent triple-band BPF for 5G applications," *International Journal of Microwave and Optical Technology*, Vol. 17, 524–532, 2022.

[9] Zhan, Y., Y. Wu, E. Fourn, P. Besnier, and K. Ma, "Synthesis and implementation of multiband SIW bandpass filters based on in-line topology," *IEEE Transactions on Microwave Theory and Techniques*, 1–14, 2024.

[10] Zhou, K. and K. Wu, "Substrate integrated waveguide multiband bandpass filters and multiplexers: Current status and future outlook," *IEEE Journal of Microwaves*, Vol. 3, No. 1, 466–483, 2022.

[11] Iqbal, A., J. J. Tiang, S. K. Wong, M. Alibakhshikenari, F. Falcone, and E. Limiti, "Miniaturization trends in substrate integrated waveguide (SIW) filters: A review," *IEEE Access*, Vol. 8, 223 287–223 305, 2020.

[12] Li, J., G. Li, Z. Wei, G. Xu, Z. Ju, and J. Huang, "Compact dual-band bandpass filter based on substrate integrated waveguide cavity with high selectivity," *Progress In Electromagnetics Research M*, Vol. 61, 147–158, 2017.

[13] Li, M., C. Chen, and W. Chen, "Miniaturized dual-band filter using dual-capacitively loaded SIW cavities," *IEEE Microwave and Wireless Components Letters*, Vol. 27, No. 4, 344–346, 2017.

[14] Azad, A. R. and A. Mohan, "Substrate integrated waveguide dual-band and wide-stopband bandpass filters," *IEEE Microwave and Wireless Components Letters*, Vol. 28, No. 8, 660–662, 2018.

[15] Zhang, H., W. Kang, and W. Wu, "Miniaturized dual-band SIW filters using E-shaped slotlines with controllable center frequencies," *IEEE Microwave and Wireless Components Letters*, Vol. 28, No. 4, 311–313, 2018.

[16] Zhang, H., W. Kang, and W. Wu, "Dual-band substrate integrated waveguide bandpass filter utilising complementary splitring resonators," *Electronics Letters*, Vol. 54, No. 2, 85–87, 2018.

[17] Azad, A. R. and A. Mohan, "Single-and dual-band bandpass filters using a single perturbed SIW circular cavity," *IEEE Microwave and Wireless Components Letters*, Vol. 29, No. 3, 201–203, 2019.

[18] Liu, Y., G. Zhang, and J. Zheng, "Compact dual-band balanced SIW bandpass filter with two adjustable closed-passbands," *Electronics Letters*, Vol. 56, No. 13, 667–669, 2020.

[19] Xie, H.-W., K. Zhou, C.-X. Zhou, and W. Wu, "Compact SIW diplexers and dual-band bandpass filter with wide-stopband performances," *IEEE Transactions on Circuits and Systems II: Express Briefs*, Vol. 67, No. 12, 2933–2937, 2020.

[20] Nosrati, A., M. Mohammad-Taheri, and M. Nosrati, "Gap-coupled dual-band evanescent-mode substrate integrated bandpass filter waveguide," *Progress In Electromagnetics Research Letters*, Vol. 89, 53–59, 2020.

[21] Zheng, Y., Z. Wang, and Y. Dong, "Compact, dual-band, and hybrid filter based on combline and substrate integrated waveguide resonators," *International Journal of RF and Microwave*

Computer-Aided Engineering, Vol. 32, No. 1, e22919, 2021.

[22] Gao, M., M. Li, J. Nan, and Y. Wang, "New dual-passband SIW filter with loaded T-slot," *Progress In Electromagnetics Research C*, Vol. 124, 243–252, 2022.

[23] Abbas, M. F. and A. J. Salim, "A new tunable dual-mode dual-band square cavity SIW bandpass filter," *Progress In Electromagnetics Research C*, Vol. 118, 113–123, 2022.

[24] Zhu, F., Y. Wu, P. Chu, G. Q. Luo, and K. Wu, "Compact dual-band filtering baluns using perturbed substrate integrated waveguide circular cavities," *IEEE Microwave and Wireless Technology Letters*, Vol. 33, No. 6, 663–666, 2023.

[25] Li, D., W. Luo, X. Chen, Y. Liu, K.-D. Xu, and Q. Chen, "Miniaturized dual-/tri-/quad-band bandpass filters using perturbed multi-mode SIW cavity," *IEEE Transactions on Components, Packaging and Manufacturing Technology*, Vol. 13, No. 10, 1685–1693, 2023.

[26] Claus, N., K. Y. Kapusuz, J. Verhaevert, and H. Rogier, "Compact and hybrid dual-band bandpass filter using folded multi-mode resonators and second-mode suppression," *Electronics*, Vol. 13, No. 10, 1921, 2024.

[27] Liu, Q., L.-S. Wu, D.-F. Zhou, K. Gong, and D.-W. Zhang, "Self-shielded single-and dual-band quad-mode substrate integrated waveguide bandpass filters based on mixed-mode cavity," *IEEE Transactions on Circuits and Systems I: Regular Papers*, Vol. 71, No. 7, 3098–3109, 2024.

[28] Cameron, R. J., C. M. Kudsia, and R. R. Mansour, *Microwave Filters for Communication Systems: Fundamentals, Design, and Applications*, John Wiley & Sons, 2018.

[29] Cassivi, Y. and K. Wu, "Low cost microwave oscillator using substrate integrated waveguide cavity," *IEEE Microwave and Wireless Components Letters*, Vol. 13, No. 2, 48–50, 2003.